Molecular Dynamics Simulation of Laser Desorption of a Fragment of Protein Kinase A from Two MALDI Matrices†

Cheng Wang and Chung F. Wong*

Department of Chemistry and Biochemistry, University of Missouri, One University Boulevard, St. Louis, Missouri 63121

Received: October 17, 2005; In Final Form: January 14, 2006

We have carried out molecular dynamics simulations to study the desorption of a dephosphorylated fragment of protein kinase A from two matrices, sinapic acid (SA) and 2,5-dihydroxybenzoic acid (DHB), after laser excitation. We have examined the results as a function of the laser fluence and of the burial depth of the guest peptide in the matrices. In most cases, we found that the energy transferred from the matrix to the guest peptide was not sufficiently large to fragment the peptide. Exceptions occurred when the peptide was more buried. This finding suggested that protein analytes might be less likely to break into smaller fragments if they were placed closer to the surface of the matrix. We have also examined how likely the guest peptide could form small clusters with the matrix molecules and found that the results depended on the degree of burial of the peptide, on the laser fluence, and on which matrix was used. Generally, stable clusters were more likely to be formed for guest peptides that were more buried, at a lower laser fluence, and in the SA rather than the DHB matrix. In addition, we found that the DHB matrix was broken down more easily by the laser than the SA matrix.

1. Introduction

Recently, matrix-assisted laser desorption ionization (MALDI) mass spectroscopy (MS) has proven to be a powerful tool for analzying large molecules such as proteins and peptides.[1] When a protein or peptide analyte is embedded in a MALDI matrix, fragmentation of the analyte is attenuated after laser irradiation so that large molecular ions can be detected in mass spectra. The microscopic mechanism of MALDI is still not well understood.[2] For example, how can the analyte escape fragmentation from the large amount of energy deposited into the system? Different models have been introduced to provide possible explanations, including those based on molecular dynamics simulations.[3−10]

Both coarse-grained and atomistic molecular dynamics simulation models have been used to simulate MALDI processes.[4−10] Coarse-grained models overcome time and length scale limitations by ignoring the atomic details of molecules. For example, in mesoscale modeling of laser ablation, each matrix molecule was approximated by a sphere so that the system size could be 20 times larger and the time scale 50 times longer than those used in atomistic simulations.[5] On the other hand, coarse-grained models ignore fine details in molecular interactions, and therefore, a number of interesting atomistic molecular dynamics simulations have also been carried out. For example, Sadeghi et al.[11] performed such simulations to study the conformational change of the guest molecule and the energy transfer between the guest and matrix after laser irradiation.

An important use of MALDI is the study of protein kinases, for example, the elucidation of their phosphorylation states. In this work, we examined a fragment of protein kinase A that can be phosphorylated to activate the enzyme. We sought to examine whether this fragment is stable in MALDI experiments utilizing a matrix formed by sinapic acid (SA) or 2,5-dihydroxybenzoic acid (DHB). These simulations could help in determining which matrices may be more suitable for analyzing such peptides in MALDI MS experiments.

TABLE 1: CHARMM Atom Types and Calculated Partial Charges for DHB

atom	atom type	partial charge	atom	atom type	partial charge
C1	CA	−0.128	O3	OH1	−0.428
C2	CA	0.225	O4	OH1	−0.420
C3	CA	−0.120	H1	HP	0.105
C4	CA	−0.143	H2	HP	0.120
C5	CA	0.277	H3	HP	0.157
C6	CA	−0.255	H4	H	0.345
C7	CD	0.633	H5	H	0.330
O1	OB	−0.495	H6	H	0.277
O2	OH1	−0.480			

Guest molecules are also often detected in complex with matrix molecules.[12,13] Here we examine whether the fragment of protein kinase A can form stable clusters with SA and DHB molecules in MALDI experiments. We also investigated whether the formation of stable clusters depended on how deeply the guest peptide was placed inside the matrix, on the laser fluence, and on which matrix was used.

Since energy flow between the matrix and guest clearly plays an important role in understanding the survival of guest molecules after laser irradiation of a guest−matrix system, further detailed analysis of energy flow in MALDI processes will be useful. In previous atomistic molecular dynamics simulations, researchers studied energy transfer by monitoring only the kinetic and internal temperature of the guest. In this work, we also analyze all the internal energy components used in a typical force field for biomolecular simulations to gain further insight. To this end, we used an energy partition scheme similar to that employed in a previous study of energy flow in proteins.[14]

We first describe our simulation model in section 2. The results will then be presented and discussed in section 3. Section 4 is the Conclusion.

† Part of the special issue "John C. Light Festschrift".

* To whom correspondence should be addressed. E-mail: wongch@umsl.edu.

10.1021/jp055939r CCC: $33.50
Published on Web 02/11/2006

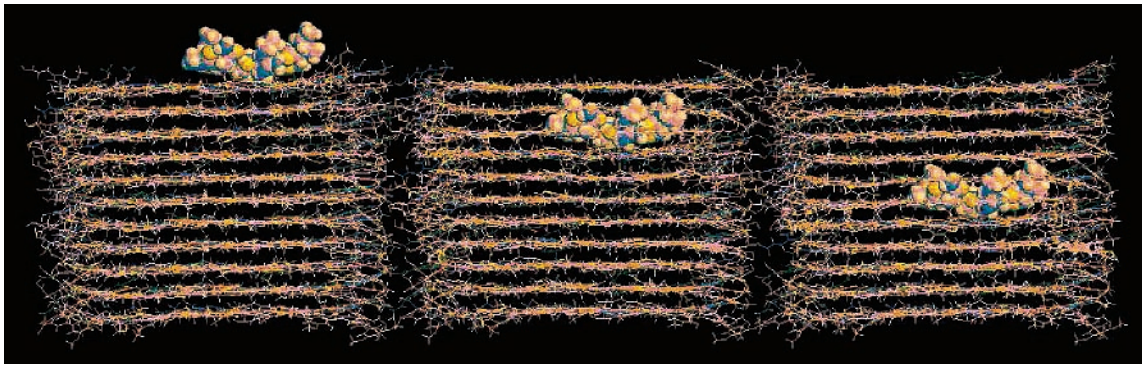

Figure 1. IRVSIN peptide placed in three different locations within the SA matrix.

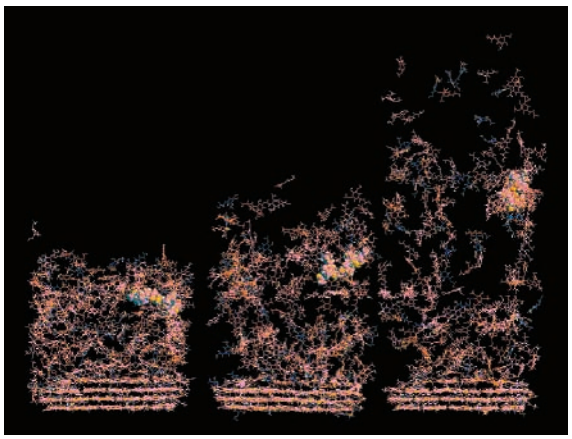

Figure 2. Snapshots of the IRVSIN peptide in the SA matrix 5, 10, and 20 ps after laser irradiation. The peptide was initially buried under three layers of matrix molecules, and the highest laser fluence (1500 K) was used.

2. Modeling Method

CHARMM was used for the simulations.[15] The CHARMM empirical potential function consists of bond, angle, dihedral, improper dihedral, van der Waals, and electrostatics terms as follows:

$$V(r_1, r_2, ..., r_N) = \sum_{\text{bonds}} k_b(b - b_0)^2 + \sum_{\text{angles}} k_\theta(\theta - \theta_0)^2 + \sum_{\text{impropers}} k_\omega(\omega - \omega_0)^2 + \sum_{\text{dihedrals}} k_\phi[1 + \cos(n\phi)] + \sum_{i,j} \left(\frac{A_{ij}}{r_{ij}^{12}} - \frac{B_{ij}}{r_{ij}^{6}}\right) + \sum_{ij} \frac{q_i q_j}{4\pi\epsilon r_{ij}}$$

Since potential parameters for the two matrices were not available in CHARMM, we carried out quantum chemical calculations to obtain partial charges and transferred other parameters from similar functional groups developed by MacKerell et al.[16,17]

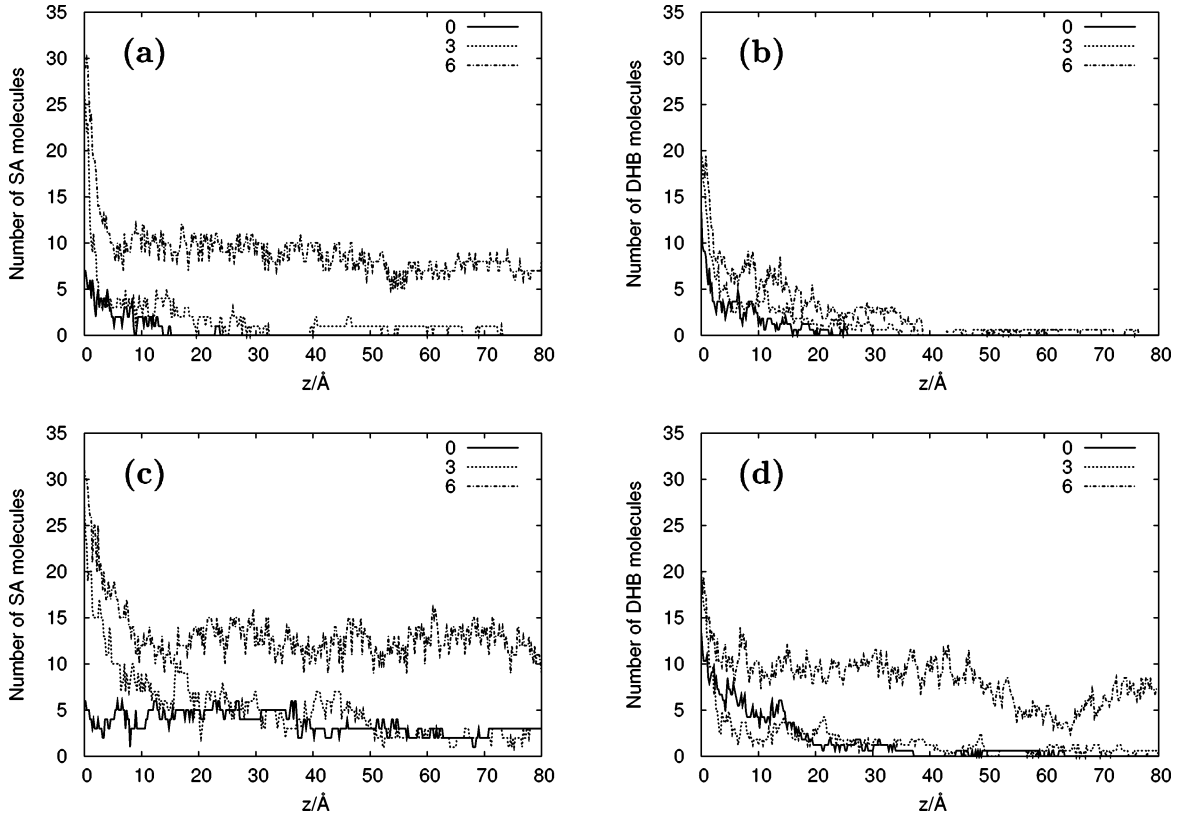

Figure 3. Number of matrix molecules within 4 Å of the guest molecule as a function of time (—, peptide initially on surface; ···, peptide initially buried by three layers of matrix molecules; -·-, peptide initially buried by six layers of matrix molecules): (a) SA matrix at 1500 K, (b) DHB matrix at 1500 K, (c) SA matrix at 1000 K, and (d) DHB matrix at 1000 K.

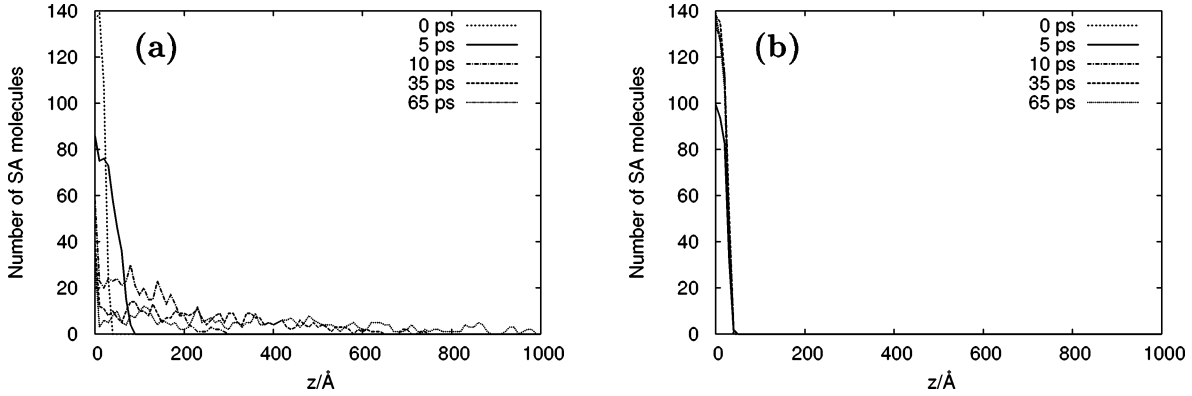

Figure 4. Structure of the SA matrix at different times at (a) 1500 and (b) 600 K. The guest molecule was initially placed under three layers of matrix molecules.

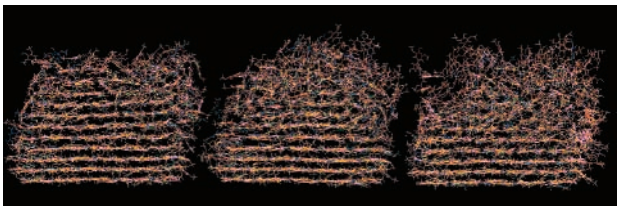

Figure 5. Structure of the SA matrix at 0, 70, and 150 ps and 600 K. The guest molecule was initially placed under three layers of matrix molecules.

The atomic partial charges of 2,5-dihydroxybenzoic acid were calculated using *Gaussian 03*[18] for the fully optimized structure at the 6-31G* level. The CHELPG option was used (see Table 1). The charges for SA were taken from ref 11.

The crystal structure of SA was built using the X-ray crystallographic structure determined by Beavis and Bridson.[19] The SA crystal was modeled by explicitly including 572 molecules, and the (103) plane was chosen as the $x-y$ plane with dimensions of 53.6742 Å × 59.039 Å. The model of the DHB crystal was built on the basis of the work of Haisa et al.′[20] The DHB crystal is monoclinic with *Pa* symmetry. The lattice parameters are as follows: $a = 11.299$ Å, $b = 11.830$ Å, $c = 4.966$ Å, and $\beta = 90.5°$. There are four molecules of DHB in the unit cell. For the DHB simulations, the (001) plane into which the guest molecule would be placed was selected as the $x-y$ plane having a cross section of 57.8961 Å × 59.162 Å. Five hundred seventy matrix molecules were included in the basic simulation unit. Crystallographic studies[19] showed that SA crystals formed hydrogen-bonding sheets along the (103) planes between which guest molecules intercalated. On the other hand, no such structures have yet been found for DHB crystals. Therefore, we placed the guest molecule on the (001) plane of the DHB crystal in this study.

The IRVSIN sequence in the activation loop of protein kinase A was used to construct a hexapeptide with the N-terminal and C-terminal ends blocked by CH_3CO (ACE) and $NHCH_3$ (CT3) groups, respectively. The serine of this sequence can be phosphorylated in protein kinase A to activate the protein. The net charge of arginine was set to +1 to be consistent with the usual acidic conditions of sample preparations.

Each crystal was first heated from 0 to 300 K in 100 ps using three-dimensional periodic boundary conditions and a time step of 1 fs. After equilibration for an additional 100 ps, during which velocities were reassigned every 1 ps, the system was allowed to evolve for an additional 100 ps by coupling to a heat bath at 300 K. To check that the potential parameters for SA and DHB were reasonable, we confirmed that the crystal structures were stable at the end of the simulations just described. Furthermore,

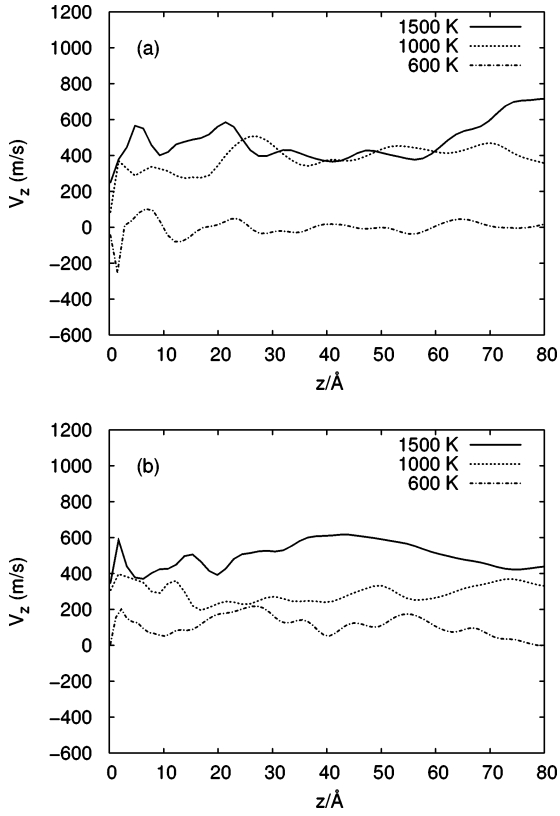

Figure 6. z component of the velocity of the center of mass of the guest peptide. The peptide was initially buried by three layers of matrix molecules: (top) SA matrix and (bottom) DHB matrix.

we calculated the densities of the simulated crystals and found them to be similar to the experimental ones. The average density of the simulated DHB crystal was 1.4725 g/cm^3, compared to the experimental value of 1.542 g/cm^3. The calculated density of the SA crystal was 1.37 g/cm^3, also quite close to the experimental value of 1.406 g/cm^3.

After equilibration of each crystal, the guest molecule was placed on the surface of the crystal according to the following procedures. We first placed the guest peptide with the extended conformation near the center of the surface. The guest was then heated to 1000 K in 100 ps with the matrix held fixed. A low-energy conformation of the guest molecule on the matrix surface was then found by cooling it to 300 K in 150 ps. The guest molecule was placed on the (103) surface of the SA crystal and the (001) surface of the DHB crystal. Two other guest−matrix structures for each matrix were constructed with the guest buried to different extents. The first was obtained by moving three

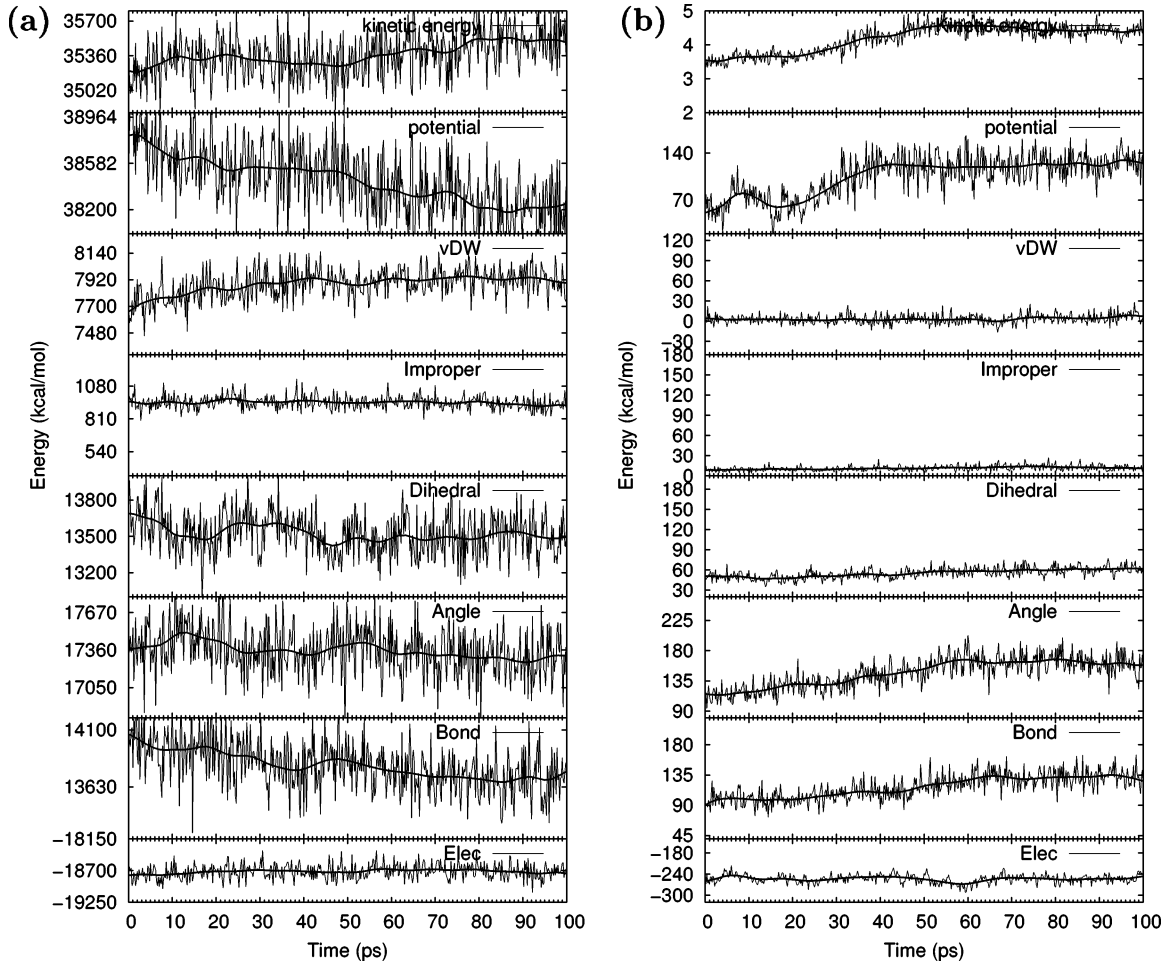

Figure 7. Time course of energy components for the SA matrix (a) and the guest peptide (b). The guest was placed on the surface of the matrix before laser irradiation at 1500 K.

layers from the bottom of the crystal to the top and removing matrix molecules within 2.4 Å of a heavy atom of the guest molecule. This system was then equilibrated for 100 ps at 300 K with two-dimensional periodic boundary conditions applied. The second structure was obtained by moving three more layers from the bottom of the matrix to the top. Again, matrix molecules within 2.4 Å of a heavy atom of the guest molecules were removed, and the system was equilibrated at 300 K for 100 ps. Figure 1 shows the three structures containing the guest peptide in the SA matrix. During the simulation of the laser ablation process, the three layers at the bottom of the crystal matrix were held fixed to mimic a bulk crystal. Three layers were chosen because it gave a thickness larger than the nonbonded cutoff distance used in the simulation (13 Å).

The laser ablation process was initiated by depositing laser energy into the matrix but not the guest molecule. This was to mimic a MALDI experiment in which the matrix absorbs most of the laser energy. As in earlier work,[11] we assumed that all the energy of a laser pulse was transferred to the kinetic energy of the matrix. However, we did this slightly differently. Instead of coupling the matrix and guest molecules to different temperature baths, we scaled the velocities of the matrix molecules according to a prescribed heating rate to simulate the heating of the matrix during the laser pulse. The heating rate was chosen to deposit the energy of a laser pulse within a time given by the pulse width. In one case, we assumed a laser fluence that could bring a guest−matrix system from 300 to 1500 K at the end of the pulse. This was done by increasing the velocity of every atom of the matrix every 500 time steps by applying the scaling factor $f_{scal} = 1 + R/E_k$, where E_k is the kinetic energy at the previous step and R was chosen such that the temperature of the matrix was increased from 300 to ∼1500 K in 15 ps, mimicking a 15 ps laser pulse. We also mimicked two lower laser fluences by heating the systems to only 600 or 1000 K.

3. Results and Discussion

Figure 2 presents the structure of the SA matrix 5, 10, and 20 ps after laser irradiation to show how it broke down. (1500 K. The guest peptide was initially buried under three layers of matrix molecules.) One can see that many matrix molecules had evaporated by 20 ps with the guest peptide carried in them. At 20 ps, the matrix molecule farthest from the bulk matrix was a factor of almost 2 of that at 5 ps. This reflects the rapid expansion of the plume after laser irradation at high fluence.

Figure 3 shows how the formation of peptide−matrix clusters depends on the burial depth, the choice of matrix, and the laser fluence. From Figure 3a, one can see that stable clusters with SA molecules were formed for only the most buried guest molecule for the highest laser fluence (1500 K) that was used. On the other hand, smaller clusters could also form for the less buried guest molecules at a lower laser fluence (1000 K, Figure 3c). It is also evident from panels b and d of Figure 3 that guest−matrix clusters did not form as well with the DHB molecules. No stable clusters were formed at the higher laser fluence, although some could still form at the lower laser fluence for the guest molecule that was most buried. Therefore, the types

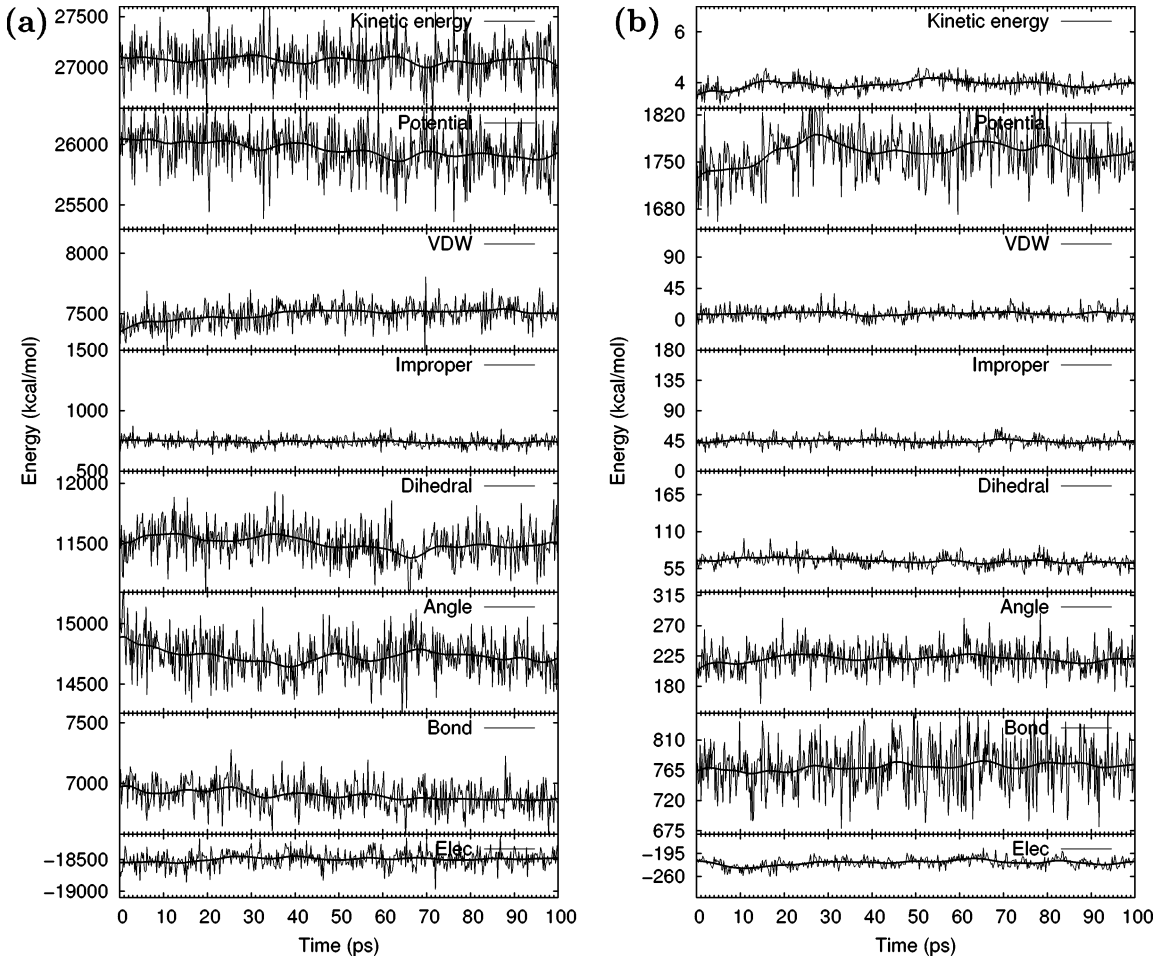

Figure 8. Time course of energy components for the SA matrix (a) and the guest peptide (b). The guest was buried within six layers of matrix molecules before laser irradiation at 1500 K.

of mass signals one can observe can depend substantially on the matrix used for MALDI MS experiments, and molecular dynamics simulations can help to predict which matrices are more likely to produce observable guest−matrix mass peaks.

Figure 4 presents a case in which the laser fluence (600 K) was not sufficiently large to break down the SA matrix. The figure plots the number of matrix molecules in 10 Å bins along the *z* direction as a means of showing how the matrix expanded after laser irradiation. Figure 4a shows the case in which a higher laser fluence (1500 K) was used in which it is clear that the matrix broke down as time progressed. Figure 4b shows the case with a lower laser fluence (600 K) in which the SA matrix expanded a bit initially but did not have enough energy to evaporate. Figure 5 shows the structure of the matrix 0, 70, and 150 ps after laser irradiation. One can see that although the SA matrix became disordered near the surface and expanded a bit, the matrix failed to break off completely to yield observable ions.

Figure 6 uses the *z* component of the velocity of the guest molecule to show how easy the two matrices broke down with different laser fluences. In Figure 6a, one can see that the matrix evaporated rapidly with the guest molecule moving fast along the *z* direction at higher laser fluences (1500 and 1000 K). However, at the lowest laser fluence that was used (600 K), the guest molecule failed to lift off with the SA matrix. It actually moved in the negative *z* direction a bit right after laser irradiation before becoming less mobile. Figure 6b shows that the DHB matrix broke down at all three laser fluences, suggesting that laser irradiation could force the DHB matrix to evaporate more easily than the SA matrix.

Figure 7 shows an example of the change in the different components of the energy as a function of time for the matrix and guest peptide when the highest laser fluence (1500 K) was used. All simulations at this laser fluence except one provided plots similar to these. They showed the general feature that as the matrix was releasing its absorbed laser energy, as indicated by the decrease in its potential energy, much of this energy was converted into its kinetic energy. As a result, very little energy was transferred to the guest peptide. The total energy (potential plus kinetic energy) of the guest peptide was increased to only ∼140 kcal/mol, ∼300 kcal/mol higher than its energy before laser irradiation. This amount of energy was smaller than that required to break approximately four bonds in the peptide. Since it was more likely to distribute this energy among the whole peptide than to focus it on only a few bonds, the chance of having enough energy to break any bond was small. This may explain why guest molecules can escape fragmentation in MALDI experiments. The only exception occurred in the simulation of the SA matrix system when the guest was most buried (by six layers of matrix molecules) (Figure 8). In this case, the guest did not lift off from the matrix during the simulation. The prolonged lifetime of the guest inside the matrix allowed much of the absorbed laser energy to be transferred from the matrix into the guest. Figures 7 and 8 also showed that the guest picked up energy mostly in its bond and angle terms than in other degrees of freedom. Therefore, for guest molecules that are more buried and if the applied laser could

not melt its surrounding matrix rapidly enough, the guest molecule could fragment even within the matrix before desorption.

4. Conclusions

We have carried out molecular dynamics simulations to study the desorption of a fragment of protein kinase A from MALDI matrices as a function of matrix, laser fluence, and burial depth. We found that the guest molecule was usually spared from fragmentation because only a small amount of the laser energy absorbed by the matrix could be transferred to the guest. This amount was usually not large enough to break bonds in the guest peptide. At 1500 K, there was only one simulation in which significant energy transfer to the guest peptide was observed. This happened in the case in which the peptide was most buried so that there was more time for the matrix to transfer its absorbed laser energy to the guest peptide. Thus, guest analytes that are less buried may provide larger ions that can be observed via mass spectrometry.

The formation of guest−matrix clusters also depended on the burial depth, the laser fluence, and the matrix. We observed that stable guest−matrix clusters were more likely to form at lower laser fluences, when the guest molecule was more buried, and for the SA than for the DHB matrix.

In addition, our model showed that the DHB matrix could be disintegrated more easily by the laser than the SA matrix.

References and Notes

(1) Berkenkamp, S.; Kirpekar, F.; Hillenkamp, F. *Science* **1998**, *281*, 260.
(2) Zenobi, R.; Knochenmuss, R. *Mass Spectrom. Rev.* **1998**, *17*, 337.
(3) Bencsura, A.; Navale, V.; Sadeghi, M.; Vertes, A. *Rapid Commun. Mass Spectrom.* **1997**, *11*, 679.
(4) Bencsura, A.; Vertes, A. *Chem. Phys. Lett. B* **1995**, *247*, 142.
(5) Zhigilei, L. V.; Kodali, P. B. S.; Garrison, B. J. *J. Phys. Chem. B* **1997**, 101, 2028; **1998**, *102*, 2845.
(6) Wu, X.; Sadeghi, M.; Vertes, A. *J. Phys. Chem. B* **1998**, *102*, 4770.
(7) Dutkiewicz, L.; Johnson, R. E.; Vertes, A.; Pedrys, R. *J. Phys. Chem. A* **1999**, *103*, 2925.
(8) Zhigilei, L. V.; Garrison, B. J. *Appl. Phys. Lett.* **1999**, *74*, 1341.
(9) Zhigilei, L. V.; Garrison, B. J. *Appl. Phys. A* **1999**, *69*, S75.
(10) Yingling, Y. G.; Garrison, B. J. *J. Phys. Chem. B* **2004**, *108*, 1815.
(11) Sadeghi, M.; Wu, X.; Vertes, A. *J. Phys. Chem. B* **2001**, *105*, 2578.
(12) Perera, I. K.; Allwood, D.; Dyer, P. E.; Oldershaw, G. A. *Int. J. Mass Spectrom. Ion Processes* **1995**, *145*, L9.
(13) Perera, I. K.; Allwood, D.; Dyer, P. E.; Oldershaw, G. A. *J. Mass Spectrom. Ion Processes* **1995**, *30*, S3.
(14) Wang, Q.; Wong, C. F.; Rabitz, H. *Biophys. J.* **1998**, *75*, 60.
(15) Brooks, B. R.; Bruccoleri, R. E.; Olafson, B. D.; Swaminathan, S.; Karplus, M. *J. Comput. Chem.* **1983**, *4*, 187.
(16) MacKerell, A. D., Jr.; Feig, M.; Brooks, C. L., III. *J. Comput. Chem.* **2004**, *25*, 1400.
(17) MacKerell, A. D., Jr.; Bashford, D.; Bellott, M.; Dunbrack, R. L., Jr.; Evanseck, J. D.; Field, M. J.; Fischer, S.; Gao, J.; Guo, H.; Ha, S.; Joseph-McCarthy, D.; Kuchnir, L.; Kuczera, K.; Lau, F. T. K.; Mattos, C.; Michnick, S.; Ngo, T.; Nguyen, D. T.; Prodhom, B.; Reiher, W. E., III; Roux, B.; Schlenkrich, M.; Smith, J. C.; Stote, R.; Straub, J.; Watanabe, M.; Wiorkiewicz-Kuczera, J.; Yin, D.; Karplus, M. *J. Phys. Chem. B* **1998**, *102*, 3586.
(18) Frisch, M. J.; Trucks, G. W.; Schlegel, H. B.; Scuseria, G. E.; Robb, M. A.; Cheeseman, J. R.; Zakrzewski, V. G.; Montgomery, J. A.; Stratmann, R. E.; Burant, J. C.; Dapprich, S.; Millam, J. M.; Daniels, A. D.; Kudin, K. N.; Strain, M. C.; Farkas, O.; Tomasi, J.; Barone, V.; Cossi, M.; Cammi, R.; Mennucci, B.; Pornelli, C.; Adamo, C.; Clifford, S.; Ochterski, J.; Petersson, J. B.; Ayala, P. Y.; Cui, Q.; Morokuma, K.; Malick, D. K.; Rabuck, A. D.; Raghavachari, K.; Foresman, J. B.; Cioslowski, J.; Ortiz, J. V.; Stefanov, B. B.; Liu, G.; Liashenko, A.; Piskorz, P.; Komaromi, A.; Gomperts, R.; Martin, R. L.; Fox, D. J.; Keith, T.; Al-Laham, M. A.; Peng, C. Y.; Nanayakkara, A.; Gonzalez, C.; Challacombe, M.; Gill, P. M. W.; Johnson, B. G.; Chen, W.; Wong, M. W.; Andres, J. L.; Head-Gordon, M.; Replogle, E. S.; Pople, J. A. *Gaussian 03*; Gaussian Inc.: Pittsburgh, PA, 2003.
(19) Beavis, R. C.; Bridson, J. N. *J. Phys. D* **1993**, *26*, 442.
(20) Haisa, M.; Kashino, S.; Hanada, S. I.; Tanaka, K.; Okazaki, S.; Shibagaki, M. *Acta Crystallogr.* **1982**, *38B*, 1480.